⌘ *Author's Choice*

THE JOURNAL OF BIOLOGICAL CHEMISTRY VOL. 284, NO. 43, pp. 29499–29508, October 23, 2009

SufA of the Opportunistic Pathogen *Finegoldia magna* Modulates Actions of the Antibacterial Chemokine MIG/CXCL9, Promoting Bacterial Survival during Epithelial Inflammation*

Received for publication, March 5, 2009, and in revised form, May 27, 2009 Published, JBC Papers in Press, July 23, 2009, DOI 10.1074/jbc.M109.025957

Christofer Karlsson[‡1], Mette Eliasson[§1], Anders I. Olin[‡], Matthias Mörgelin[‡], Anna Karlsson[¶], Martin Malmsten[‖], Arne Egesten[§], and Inga-Maria Frick[‡2]

From the Divisions of [‡]Infection and [§]Respiratory Medicine, Department of Clinical Sciences Lund, Lund University, SE-221 84 Lund, the [¶]Department of Rheumatology and Inflammation Research, University of Göteborg, SE-413 46 Göteborg, and the [‖]Department of Pharmacy, Uppsala University, SE-751 23 Uppsala, Sweden

The anaerobic bacterium *Finegoldia magna* is part of the human commensal microbiota, but is also an important opportunistic pathogen. This bacterium expresses a subtilisin-like serine proteinase, SufA, which partially degrade the antibacterial chemokine MIG/CXCL9. Here, we show that MIG/CXCL9 is produced by human keratinocytes in response to inflammatory stimuli. In contrast to the virulent human pathogen *Streptococcus pyogenes*, the presence of *F. magna* had no enhancing effect on the MIG/CXCL9 expression by keratinocytes, suggesting poor detection of the latter by pathogen-recognition receptors. When MIG/CXCL9 was exposed to SufA-expressing *F. magna*, the molecule was processed into several smaller fragments. Analysis by mass spectrometry showed that SufA cleaves MIG/CXCL9 at several sites in the COOH-terminal region of the molecule. At equimolar concentrations, SufA-generated MIG/CXCL9 fragments were not bactericidal against *F. magna*, but retained their ability to kill *S. pyogenes*. Moreover, the SufA-generated MIG/CXCL9 fragments were capable of activating the angiostasis-mediating CXCR3 receptor, which is expressed on endothelial cells, in an order of magnitude similar to that of intact MIG/CXCL9. *F. magna* expresses a surface protein called FAF that is released from the bacterial surface by SufA. Soluble FAF was found to bind and inactivate the antibacterial activity of MIG/CXCL9, thereby further potentially promoting the survival of *F. magna*. The findings suggest that SufA modulation of the inflammatory response could be a mechanism playing an important role in creating an ecologic niche for *F. magna*, decreasing antibacterial activity and suppressing angiogenesis, thus providing advantage in survival for this anaerobic opportunist compared with competing pathogens during inflammation.

The mucosal surfaces and skin of the human body are colonized by a large number of bacterial species constituting the normal microbiota. In contrast to pathogens, these commensals usually do not elicit any inflammatory responses in epithelial tissues of the healthy host (1). The Gram-positive coccus *Finegoldia magna* is part of the anaerobic normal microbiota associated with the skin (2), but it also inhabits the oro-pharynx, gastrointestinal, and urogenital tracts (3). During disturbed homeostasis, this bacterium becomes an important opportunistic pathogen; associated with several clinical conditions, such as soft tissue infections, wound infections, bone/joint infections, and vaginosis (3–5). Among anaerobic cocci of the normal microbiota, *F. magna* is the species most commonly isolated from clinical conditions (3).

Recognition of bacteria and their products by cells residing in the submucosal tissues, for example dendritic cells, triggers an inflammatory response leading to production of host defense molecules, including chemokines. Chemokines comprise a large family of peptides that are key players in inflammation by regulating leukocyte trafficking and activation. They are divided into four groups, XC, CC, CXC, and CX_3C, depending on the arrangement of conserved cysteine residues in their NH_2 terminus (6). The CXC subfamily can be further divided into ELR-positive and ELR-negative respectively, based on the presence or absence of the sequence motif glutamic acid-leucine-arginine (ELR) NH_2 terminal to the first cysteine. IFN-γ, a key cytokine produced during bacterial infection, induces expression of the ELR-negative CXC-chemokine MIG/CXCL9 (Monokine Induced by Gamma-interferon)[3] (7). MIG/CXCL9 binds and activates a G-protein-coupled seven transmembrane receptor, CXCR3, which is present on eosinophils, activated T cells (CD8+), and NK cells (8). In addition to its ability to recruit and activate leukocytes, MIG/CXCL9 possesses angio-

* This work was supported by grants from the Swedish Research Council (Projects 7480, 2007-2880, and 621-2003-4022), the Swedish Heart and Lung Foundation, the Medical Faculty at Lund University, the Foundations of Bergh, Bergvall, Crafoord, Ihre, Hedberg, Kock, O. E. and Edla Johansson, Marcus and Marianne Wallenberg, and Österlund, and Hansa Medical AB.

⌘ *Author's Choice*—Final version full access.

[1] Both authors contributed equally to this work.

[2] To whom correspondence should be addressed: BMC B14, Tornavägen 10, SE-221 84 Lund, Sweden. Tel.: 46-46-222-8569; Fax: 46-46-15-7756; E-mail: Inga-Maria.Frick@med.lu.se.

[3] The abbreviations used are: MIG/CXCL9, monokine-induced by γ-interferon/CXCL9; FAF, *F. magna* adhesion factor; SufA, Subtilase of *Finegoldia magna*; TH, Todd-Hewitt broth; cfu, colony forming unit; K-SFM, keratinocyte serum-free medium; Q-PCR, quantitative real-time PCR; MS, mass spectrometry; MS/MS, tandem mass spectrometry; CF, carboxyfluorescein; TLRs, toll-like receptors; ACN, acetonitrile; IFN, interferon; PMSF, phenylmethylsulfonyl fluoride; GST, glutathione *S*-transferase; Tricine, *N*-[2-hydroxy-1,1-bis(hydroxymethyl)ethyl]glycine; MALDI-TOF, matrix-assisted laser desorption/ionization-time of flight.

static properties through activation of CXCR3 expressed on endothelial cells, and it also exerts potent antibacterial properties (9–11). Upon IFN-dependent inflammation, for example during bacterial infection, this chemokine is produced by epithelial cells and participates in activities of both innate and adaptive immunity (10, 12–14).

The finding that epithelial cells recognize important human pathogens, such as *Streptococcus pyogenes*, leading to an increased MIG/CXCL9 production (10, 12) raised the question whether an opportunistic pathogen like *F. magna* could be recognized in a similar fashion. In skin *F. magna* is localized to the epidermis where they adhere to basement membranes through an interaction with the basement membrane protein BM-40 (15). Binding to BM-40 is mediated by the surface protein FAF (F. magna adhesion factor) that is expressed by more than 90% of *F. magna* isolates (15). Bacteria, both commensals and pathogens, express proteases that are important both during colonization and invasion (16). In the case of *F. magna*, most strains express a subtilisin-like enzyme, SufA (Subtilase of Finegoldia magna), which is associated with the bacterial surface, but also secreted in substantial amounts during bacterial growth (17). Studies on the proteolytic activity of SufA demonstrated that the enzyme cleaves and inactivates antibacterial molecules like LL-37 and MIG/CXCL9 (17). Here, we show that MIG/CXCL9, produced by human keratinocytes in response to inflammatory stimuli, is degraded by SufA-expressing *F. magna*. The generated MIG/CXCL9 fragments are still able to activate the MIG/CXCL9 receptor, CXCR3 and kill *S. pyogenes*, while *F. magna* is left unaffected. This modulation of the MIG/CXCL9 activities promotes the survival of *F. magna* during inflammation.

EXPERIMENTAL PROCEDURES

Special Reagents and Cleavage of MIG/CXCL9—Native SufA was purified from strain ALB8 as previously described (17). Recombinantly expressed protein FAF (amino acids 28–616), the NH_2 terminus (amino acids 28–317), and the COOH terminus (amino acids 239–616) fragments of FAF were obtained in fusion with GST (the GST tag removed with Prescission protease) as described previously (15). Rabbit anti-FAF antibodies were raised against recombinant FAF (15). Recombinant human IFN-γ, MIG/CXCL9, and affinity-purified polyclonal rabbit antibodies against human MIG/CXCL9 were from Peprotech. ELISA for the detection of MIG/CXCL9 was obtained from R&D Systems. MIG/CXCL9 (3 μg) was incubated with SufA (100 ng) for 3 h at 37 °C, and peptide degradation analyzed on Tris-Tricine peptide gels (see below).

Bacterial Strains, Growth Conditions, and FAF Release—*F. magna* clinical strains ALB8 and 505 were from Lund University Hospital, Lund, Sweden, while the mutant CK05 has been described earlier (18). *S. pyogenes* strain AP1 (40/58) of serotype M1 was from the WHO Collaborating Centre for Reference and Research on Streptococci, Prague, Czech Republic. AP1 was grown in Todd-Hewitt broth (TH; Difco) at 37 °C, 5% CO_2. *F. magna* strains were grown in TH supplemented with 0.5% Tween-80 at 37 °C under strict anaerobic conditions (Anaerobic Work station, Elektrotek). For cultivation of CK05, 200 μg/ml kanamycin was added. ALB8 bacteria were cultivated for 3 days, harvested by centrifugation at 5000 × *g* for 30 min, washed with 20 mM Tris-HCl, pH 7.5, and adjusted to a concentration of 1% (2×10^9 colony forming units (cfu)/ml). Bacterial solutions were left at 4 °C or 37 °C with buffer, SufA, or SufA in presence of PMSF (Sigma) for 3 h and then vortexed for 60 s. Supernatants were collected by centrifugation and filter-sterilized through 0.22-mm membranes.

Cell Culture and Stimulation of Cells—HaCaT cells, a spontaneously transformed non-tumorigenic keratinocyte cell line derived from adult human skin (19), were cultured in keratinocyte serum-free medium (K-SFM) (Invitrogen) supplemented with 5 μg/ml recombinant human EGF (Invitrogen), 50 μg/ml bovine pituitary extract (Invitrogen), and 650 ng/ml gentamicin. Cells were cultivated in 25 cm^2 cell culture flasks at 37 °C in an atmosphere containing 5% CO_2 with 100% relative humidity. Experiments were carried out in 24-well plates when cells were close to confluent. Cell culture flasks and plates were from NUNC. HaCaT cells were incubated with IFN-γ (100 units/ml) in K-SFM for 24 h. The concentration of MIG/CXCL9 in the cell supernatants was determined by ELISA. For stimulation with bacteria, 2×10^7 cfu were added to the cells. Following cultivation for various time points, the conditioned medium was collected, sterile-filtered, precipitated with acetone, and analyzed by Western blot. Cells were also collected for RNA extraction (see below).

CXCR3 Transfectants and Measurement of Calcium Flux—The murine pre-B cell line L1.2, stably expressing CXCR3, and non-transfected cells serving as control, were employed for calcium measurement, reflecting activation of the receptor (kindly provided by Dr. Bernhard Moser, The Theodor Kocher Institute, University of Bern, Switzerland). Cells at a density of 2×10^7/ml in Ca^{2+}-free KRG (Krebs-Ringer phosphate buffer containing glucose (10 mM), Mg^{2+} (1.5 mM), pH 7.3) supplemented with bovine serum albumin (0.1%) were incubated with the acetoxymethylated derivative Fura-2/AM (2 mM) at room temperature for 30 min. The cells were washed twice and resuspended in KRG, adjusted to 2×10^7/ml, and kept protected from light on ice until use. Cells were equilibrated for 5 min at 37 °C, after which the peptide agonist was added. Fura-2 fluorescence was followed with a luminescence spectrometer (LS50B; PerkinElmer) using excitation wavelengths of 340 nm and 380 nm, and an emission wavelength of 510 nm. The intracellular concentration of Ca^{2+} was calculated as described earlier (20). Maximal and minimal values were determined in presence of Triton X-100 and EGTA/Tris-HCl, respectively.

Quantitative Real-time RT-PCR (Q-PCR)—At different time points, total cellular RNA was isolated from the HaCaT cells using RNeasy RNA purification kit (Qiagen). cDNA was synthesized from RNA using iScript cDNA Synthesis kit (Bio-Rad) with 400 ng of total RNA as template in a total reaction volume of 20 μl. Q-PCR was run with iQ SYBR Green Supermix (Bio-Rad), in a total reaction volume of 20 μl, using a iQ5 Real-time Detection System (Bio-Rad). The housekeeping gene GAPDH was chosen as endogenous control throughout the experiments. The labeled MIG/CXCL9 primers were from Applied Biosystems. All Q-PCR experiments were performed following

the general guidelines from Bio-Rad. All samples were analyzed in triplicates.

SDS-PAGE and Western Blot—SDS-PAGE was performed as described by Laemmli (21) using a total polyacrylamide concentration of 10%, and 3.3% cross-linking. Analysis of peptide degradation was performed with Tricine-SDS-PAGE (22) using a polyacrylamide concentration of 16.5% and 3.3% cross-linking. Gels were either stained with Coomassie R-250 or, in the case of Western blot, the separated proteins were transferred onto an Immobilon-P membrane (Millipore) using the Mini Trans-Blot system (Bio-Rad). For Western blot, MIG/CXCL9 was detected with polyclonal rabbit antibodies (final concentration 0.2 μg/ml) and FAF detected with polyclonal rabbit anti-FAF antiserum (1:1000). Bound antibodies were detected by using horseradish peroxidase-conjugated goat anti-rabbit IgG (Bio-Rad) and visualized using Supersignal West Pico chemiluminescent substrate (Pierce).

Determination of SufA Cleavage Sites by MALDI-TOF Mass Spectrometry (MS) and HPLC-Q-TOF MS/MS—MIG/CXCL9 incubated with SufA (see above) was separated by SDS-PAGE and visualized by Coomassie Blue staining. Gel pieces were excised and washed four times with 40% (v/v) acetonitrile (ACN). Thereafter, they were evaporated to dryness, and reduction of MIG/CXCL9 fragments generated by SufA cleavage was carried out in 10 mM dithiothreitol at 56 °C for 30 min. Superfluous solution was aspirated and the peptides alkylated with 30 mM iodoacetamide in the dark at room temperature. Then, the gel pieces were washed as above and again evaporated to dryness. The peptides were further degraded into characteristic fragments with Asp-N + N-terminal Glu according to the manufacturer's instructions. Peptides were purified using C18 Ziptips™ (Millipore) and applied to a MALDI Anchorchip™ target plate (Bruker Daltonic GmbH, Germany) pre-spotted with 2,5-dihydroxy-benzoic acid matrix as previously described (23).

The MALDI target was loaded into a Bruker Reflex™ III MALDI-TOF mass spectrometer (Bruker Daltonic GmbH, Germany). The polarity of the instrument was set for positive ions with a delayed extraction and the detector for reflector mode. The acceleration voltage was 20 kV and 50 shots per sample were summed in each spectrum for an improved signal-to-noise ratio. Spectra were calibrated using mixture standards diluted to 1–2 μM and applied as above in 1 μl of 90% ACN/0.1% trifluoroacetic acid. Evaluated machine-specific protocols and settings for the mass spectrometer were used. During evaluation of data, mass tolerance was set to $\pm$ 0.5 Da, cysteines taken to be reduced, and methionines as well as tryptophans as oxidized. For peptide sequencing, the samples (from above and from a parallel trypsin (porcine, sequencing grade, Promega) digestion performed on gel pieces as above) were analyzed on a Q-TOF Ultima API ESI-MS/MS (electrospray ionization) coupled to a CapLC HPLC (Waters, Manchester, UK). Peptides were trapped on a pre-column (C18, 300 μm $\times$ 5 mm, 5 μm, 100 Å, LC-Packings), and separated on a reversed phase analytical column (C18, 75 μm $\times$ 150 mm, 3 μm, 100 Å, Waters) at 200 nl/min in 2–90% ACN/0.1% formic acid over a total gradient run of 90 min.

The analysis was made by Data Dependent Acquisition. The mass range m/z was from 400 to 1600 for MS and from 50 to 1800 for MS/MS. Only spectra from ions with charge state 2 and 3 were acquired. Obtained amino acid sequences were compared with MIG/CXCL9 and to the MALDI-TOF mapping of cleavage products by molecular weight.

Amino Acid Sequencing Analysis—Samples subjected to NH_2 terminus amino acid sequencing were separated by SDS-PAGE, stained with Coomassie Blue and protein bands cut out from the gel. Sequencing was performed at the Protein Analysis Center (PAC) at Karolinska Institutet, Stockholm, Sweden.

Modeling a Predictive Structure of MIG/CXCL9—A homology model of MIG/CXCL9 was generated using Multiple Mapping Method with Multiple Templates (M4T) (24) using NAP-2/CXCL7 (PDB1TVX) (25) as a template. The MIG/CXCL9 model was visualized using VMD 1.8.6 (26) and high resolution images were generated using the Tachyon ray tracer (27).

Bactericidal Assay—Stationary phase *F. magna* bacteria (strain 505) were washed with 10 mM Tris/HCl, 5 mM glucose, pH 7.5 (incubation buffer), and adjusted to a concentration of 2×10^6 cfu/ml. 50 μl of the bacterial solution ($\sim 10^5$ cfu) was incubated with various concentrations of MIG/CXCL9 or SufA-cleaved MIG/CXCL9 for 1 h under strict anaerobic conditions. To quantify the bactericidal activity, serial dilutions of the mixtures were plated on TH agar in duplicates and incubated at 37 °C for 3 days under anaerobic conditions. The number of cfus was then determined. In subsequent experiments, bacteria were incubated with MIG/CXCL9 (0.28 μM) together with various concentrations of FAF, and the bactericidal activity was determined as above. *S. pyogenes* strain AP1 was cultivated in TH to mid-exponential growth phase (OD_{620} = 0.4). The bacteria were washed, diluted in incubation buffer, and approximately 10^5 cfu were incubated with MIG/CXCL9 or SufA-cleaved MIG/CXCL9 for 1 h at 37 °C. The mixtures were diluted, plated on TH-agar, incubated at 37 °C overnight, and the number of cfu counted. All dilutions were performed in incubation buffer.

The conditioned medium from stimulated HaCaT cells (antibiotic-depleted) were used in the antibacterial assay. 25 μl of AP1 bacteria at mid-exponential growth phase ($\sim 0.5 \times 10^5$ cfu) were washed, diluted in incubation buffer, and incubated with 25 μl of cell supernatant for 1 h at 37 °C. The number of viable bacteria able to form colonies was determined as above.

Surface Plasmon Resonance Spectrometry—Protein FAF was immobilized via amine coupling in flow cells of a CM5 sensorchip (BIAcore AB, Uppsala, Sweden). The immobilization level was ~1 000 resonance units. A flow cell subjected to the coupling reaction without added protein was used as control for bulk refractive index changes. For affinity measurements, binding and dissociation were monitored in a BIAcore 2000 instrument. Different concentrations of MIG/CXCL9 were injected over the coated surface at 10 μl/min and 25 °C (in running buffer: 10 mM Hepes, pH 7.5, 150 mM NaCl, 0.005% surfactant P20, and 3.4 mM EDTA). The FAF surface was regenerated by injection of a 200 μl 2-min pulse of running buffer containing 2 M NaCl followed by an extensive wash procedure. After X and Y normalization of data, the blank curves from the control flow cell of each injected concentration were subtracted. The asso-

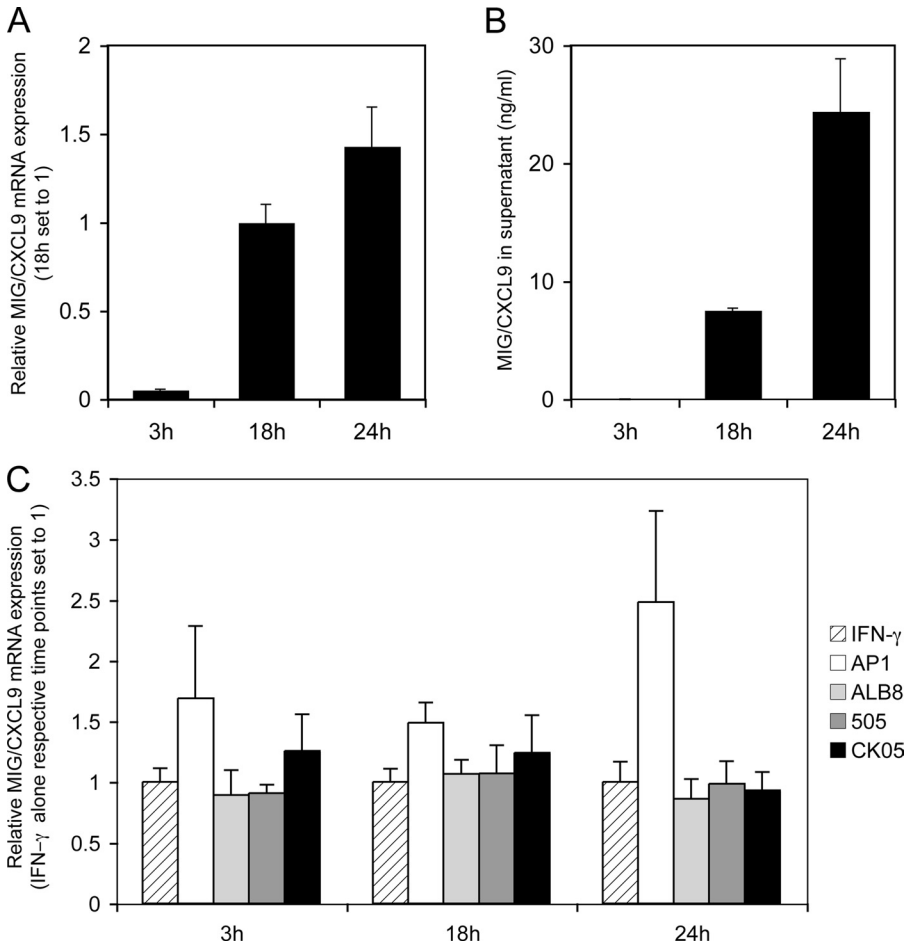

FIGURE 1. **Human keratinocytes produce MIG/CXCL9 in response to inflammatory stimuli.** *A*, HaCaT cells were stimulated with IFN-γ (100 units/ml). At indicated time points, RNA was isolated from the cells and MIG/CXCL9 gene expression quantified using Q-PCR. The data shown represent relative MIG/CXCL9 gene expression, where the expression at 18 h is set to a value of 1. GAPDH was used as housekeeping gene to normalize the values obtained, and each sample was analyzed in triplicate. *B*, MIG/CXCL9 peptide concentration in medium from HaCaT cells used for RNA isolation in *A*. Supernatants were collected, and the MIG/CXCL9 content was measured by ELISA. *C*, HaCaT cells were stimulated with IFN-γ (100 units/ml) in presence of *F. magna* strains 505, ALB8, and CK05 (expressing a truncated inactive form of SufA), or the *S. pyogenes* strain AP1 (2×10^7 cfu/ml). RNA was isolated from the cells, and the MIG/CXCL9 gene expression quantified using Q-PCR. Relative gene expression of MIG/CXCL9 is shown and the expression, at the individual time points, are compared with cells stimulated with IFN-γ alone, where the values was set to 1 at respective time points.

ciation (k_a) and dissociation (k_d) rate constants were determined simultaneously using the equation for 1:1 Langmuir binding in the BIA Evaluation 3.1 software (BIAcore). The binding curves were fitted locally and the equilibrium dissociation constants (K_D) were calculated from mean values of the obtained rate constants.

Liposome Preparation and Leakage Assay—The liposomes investigated were anionic (DOPE/DOPG 75/25 mol/mol). DOPG (1,2-dioleoyl-*sn*-glycero-3-phosphoglycerol, monosodium salt) and DOPE (1,2-dioleoyl-*sn*-glycero-3-phosphoethanolamine) were from Avanti Polar Lipids (Alabaster) and of >99% purity. The lipid mixtures were dissolved in chloroform, after which solvent was removed by evaporation under vacuum overnight. Subsequently, 10 mM Tris buffer, pH 7.4, was added together with 0.1 M carboxyfluorescein (CF) (Sigma). After hydration, the lipid mixture was subjected to eight freeze-thaw cycles consisting of freezing in liquid nitrogen and heating to 60 °C. Unilamellar liposomes of about Ø140 nm were generated by multiple extrusions through polycarbonate filters (pore size 100 nm) mounted in a LipoFast miniextruder (Avestin, Ottawa, Canada) at 22 °C. Untrapped CF was removed by two subsequent gel filtrations (Sephadex G-50, GE Healthcare, Uppsala, Sweden) at 22 °C, with Tris buffer as eluent. CF release from the liposomes was determined by monitoring the emitted fluorescence at 520 nm from a liposome dispersion (10 mM lipid in 10 mM Tris, 5 mM glucose, pH 7.5). An absolute leakage scale was obtained by disrupting the liposomes at the end of each experiment through addition of 0.8 mM Triton X-100 (Sigma). A SPEX-fluorolog 1650 0.22-m double spectrometer (SPEX Industries, Edison) was used for the liposome leakage assay. Measurements were performed in duplicate at 37 °C.

CD Spectroscopy—Circular dichroism (CD) spectra were measured by a Jasco J-810 Spectropolarimeter (Jasco, Easton, USA). The measurements were performed in triplicate at 37 °C in a 5-mm quartz cuvette under stirring with a peptide concentration of 1 μM (MIG/CXCL9), equivalent of 1 μM degraded sample (MIG/CXCL9 + SufA), and 0.30 ng/μl (SufA). The effect on peptide secondary structure of liposomes at a lipid concentration of 100 μM was monitored in the range 200–250 nm. To account for instrumental differences between measurements, the background value (detected at 250 nm, where no peptide signal is present) was subtracted. Signals from the bulk solution were also corrected for.

Electron Microscopy—1-ml solution of *F. magna* ALB8 and *S. pyogenes* AP1 bacteria (2×10^9 cfu in 10 mM Tris/HCl, 5 mM glucose, pH 7.5) were incubated with MIG/CXCL9 (5 μg) and SufA-cleaved MIG/CXCL9 (5 μg) for 1 h at 37 °C. Bacteria were collected by centrifugation at 5000 × *g* at 4 °C and prepared for electron microscopy by addition of fixative (1.5% paraformaldehyde + 0.5% glutaraldehyde in 0.1 M phosphate buffer, pH 7.4) for 1 h at room temperature and washed with 0.1 M phosphate buffer, pH 7.4. The fixed and washed pellets were subsequently dehydrated in ethanol and further processed for Lowicryl embedding (28). Sections were cut with a LKB ultratome and mounted on gold grids.

For immunostaining, grids were floated on top of drops of immune reagents displayed on a sheet of parafilm. Free aldehyde groups were blocked with 50 mM glycine in phosphate-buffered saline (PBS), and followed by incubation with 5% (v/v)

goat serum in incubation buffer (0.2% bovine serum albumin-c in PBS, pH 7.6) for 15 min. This blocking procedure was followed by overnight incubation with polyclonal rabbit anti-human MIG/CXCL9 (1 μg/ml) at 4 °C. After washing the grids in a large volume (200 ml) of incubation buffer, floating on drops containing gold-conjugated reagent (goat anti-rabbit IgG 1 μg/ml in incubation buffer, 10 nm Au) was performed for 2 h at 4 °C. After further washes in a large volume of incubation buffer, the sections were postfixed in 2% glutaraldehyde. Finally, sections were washed with distilled water, poststained with 2% uranyl acetate and lead citrate, and examined with a Jeol JEM 1230 electron microscope operated at 80 kV accelerating voltage. Images were recorded with a Gatan Multiscan 791 charge-coupled device camera.

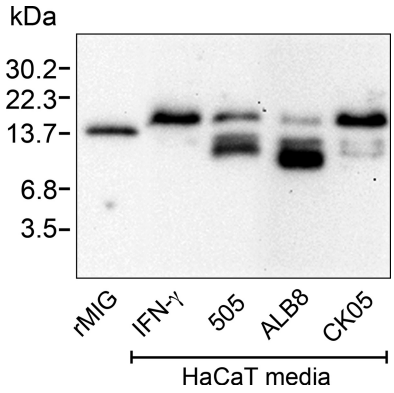

FIGURE 2. **SufA-expressing strains of *F. magna* degrade MIG/CXCL9 produced by IFN-γ-stimulated keratinocytes.** HaCaT cells were stimulated with IFN-γ alone (100 units/ml) or together with *F. magna* strains 505, ALB8, and CK05 (2×10^7 cfu). After 24 h, the cell culture media were collected, precipitated, and analyzed by Western blot using a polyclonal rabbit antibody against human MIG/CXCL9 (0.2 μg/ml). Recombinant MIG/CXCL9 (rMIG, 100 ng) was used as control.

RESULTS

SufA Cleaves MIG/CXCL9 Produced by Keratinocytes—To analyze the production of MIG/CXCL9 by inflamed human keratinocytes, a human keratinocyte cell line (HaCaT) was stimulated with IFN-γ, the latter a key cytokine in the inflammatory response during bacterial infection. Following stimulation of cells with IFN-γ for 3, 18, and 24 h, respectively, RNA was isolated, translated to cDNA, and quantitative real-time PCR (Q-PCR) was performed to investigate the levels of MIG/CXCL9 transcription. The gene expression was found to increase with time (Fig. 1*A*) and a parallel increase in the concentration of MIG/CXCL9 peptide was detected in the cell cul-

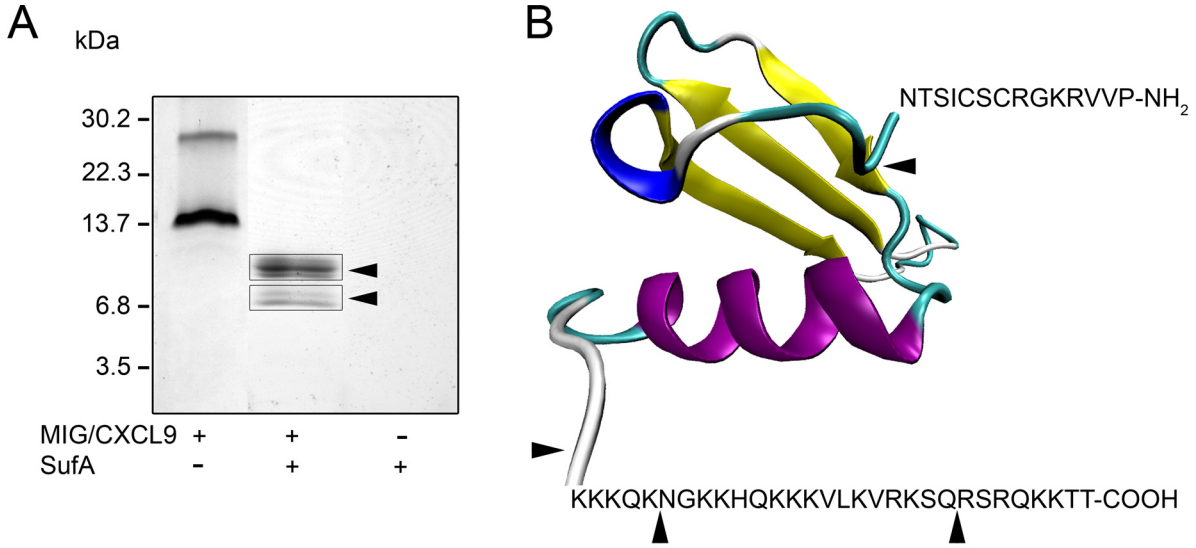

C

```
TPVVRKGRCSCISTNQGTIHLQSLKDLKQFAPSPSCEKIEIIATLKNGVQTCLNPDSADVKELIKKWEKQVSQKKKQKNGKKHQKKKVLKVRKSQRSRQKKTT

                  TIHLQSLKDLKQFAPSPSCEKIEIIATLKNGVQTCLNPDSADVKELIKKWEKQVSQKKKQKNGKKHQKKKVLKVRKSQ  8950.6
TPVVRKGRCSCISTNQGTIHLQSLKDLKQFAPSPSCEKIEIIATLKNGVQTCLNPDSADVKELIKKWEKQVSQKKKQK 8722.2
TPVVRKGRCSCISTNQGTIHLQSLKDLKQFAPSPSCEKIEIIATLKNGVQTCLNPDSADVKELIKKWEKQ 7767.0
                  TIHLQSLKDLKQFAPSPSCEKIEIIATLKNGVQTCLNPDSADVKELIKKWEKQVSQKKKQK 6934.1
                  TIHLQSLKDLKQFAPSPSCEKIEIIATLKNGVQTCLNPDSADVKELIKKWEKQ 5978.9
```

FIGURE 3. **Identification of the SufA cleavage sites in MIG/CXCL9.** *A*, recombinant MIG/CXCL9 (3 μg) was incubated with buffer or SufA (100 ng) for 3 h at 37 °C. Thereafter, samples were run on a 16.5% Tris-Tricine gel. *Lane 1*, intact MIG/CXCL9; *lane 2*, SufA degraded MIG/CXCL9; *lane 3*, SufA alone. Protein bands in *lane 2* were excised and analyzed using MS and MS/MS. *B*, visualization of a homology model of MIG/CXCL9 using NAP-2/CXCL7 as a template. β-Strands are shown in *yellow*, α-helices in *purple*, 3_{10}-helices in *blue*, and loops in *turquoise*. The amino acid sequences shown correspond to the flexible NH_2-terminal and COOH-terminal ends of MIG/CXCL9 that are not included in the model. *Arrowheads* indicate predicted cleavage sites for SufA. *C*, amino acid sequence of MIG/CXCL9 holopeptide is shown at the *top*, with the identified bactericidal region (10) in *bold/underlined*. The sequences shown *below* correspond to the peptide sequences present in the SufA-cleaved MIG/CXCL9, as determined by MS and MS/MS analysis. From the peptide masses matching with the MIG/CXCL9 sequence, the tools "Peptidecutter" and "Findpept" were used to search for experimentally (Asp-N + N-terminal Glu) as well as SufA-generated cleavage sites. Peptides matching a known cleavage site in one terminal and an unknown site in the other terminal were considered as relevant, if identified in three successive experiments. Results were further confirmed by MS/MS identification of sequence stretches within the different fragments. *Arrowheads* point at predicted cleavage sites for SufA.

ture medium by ELISA (Fig. 1*B*). Receptors of the innate immune system, *e.g.* Toll-like receptors (TLRs), on epithelial cells can recognize bacterial cell wall components, leading to increased expression of MIG/CXCL9 via activation of the NF-κB pathway (29). Therefore, the effect of *F. magna* on MIG/CXCL9 expression was investigated. Keratinocytes were stimulated with IFN-γ in the presence of the SufA-expressing *F. magna* strains 505 and ALB8, respectively, or the strain CK05 that expresses a truncated, inactive form of SufA (18). The surface protein FAF that mediates adhesion of *F. magna* to epidermal tissue is expressed by ALB8 and CK05, while 505 bacteria lack this protein (15). As shown in Fig. 1*C*, none of the strains had any enhancing effect on MIG/CXCL9 expression. In contrast, an isolate of the virulent pathogen *S. pyogenes* (strain AP1) enhanced the transcription of MIG/CXCL9 (Fig. 1*C*).

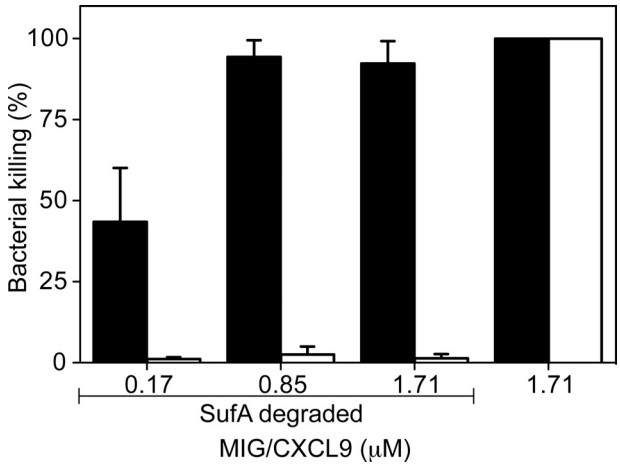

FIGURE 4. **Antibacterial effect of SufA degraded MIG/CXCL9.** Recombinant MIG/CXCL9 (3 μg) was incubated with SufA (100 ng) for 3 h at 37 °C. Indicated concentrations of intact and SufA-degraded MIG/CXCL9 were then incubated with 50 μl of a bacterial solution (2×10^6 cfu/ml) for 1 h at 37 °C. *White bars*, *F. magna* 505; *black bars*, *S. pyogenes* AP1. Bacterial killing (percent) was determined by comparing the number of bacterial colonies after exposure to MIG/CXCL9 with the number obtained after incubation in buffer alone. Data are values from three separate experiments.

In an earlier study, we demonstrated that purified SufA cleaves MIG/CXCL9 (17). To investigate if this is also the case when SufA-expressing *F. magna* infect human keratinocytes, HaCaT cells were stimulated with IFN-γ in the presence of strains 505, ALB8, or CK05, for 24 h. The supernatants were collected and, after concentration, analyzed by Western blotting, using antibodies against MIG/CXCL9. In supernatants from cells infected with the SufA-expressing strains 505 and ALB8, MIG/CXCL9 was cleaved, while in the supernatant from the mutant strain CK05, no major cleavage occurred, demonstrating the dependence on SufA (Fig. 2). The faint smaller bands seen in the supernatant from cells infected with CK05 most likely correspond to spontaneous hydrolysis of MIG/CXCL9 as such cleavage is also observed in the control with IFN-γ alone.

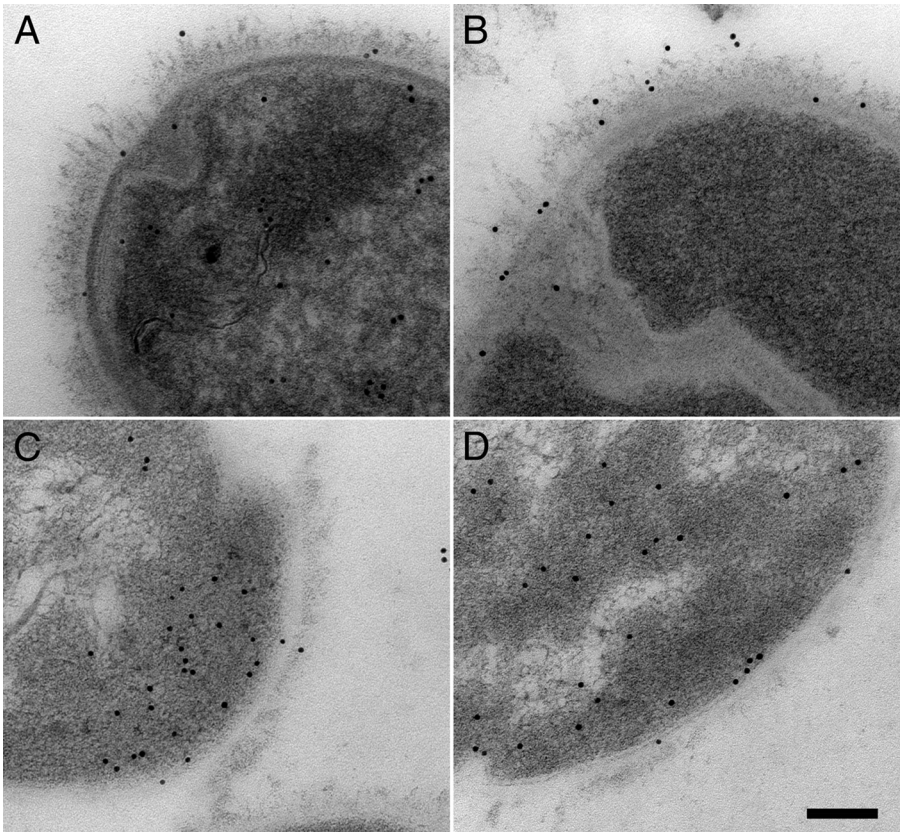

FIGURE 5. **Electron micrographs of *S. pyogenes* and *F. magna* incubated with MIG/CXCL9.** *F. magna* 505 (*A* and *B*) and *S. pyogenes* AP1 (*C* and *D*) (2×10^9 cfu/ml) were incubated with MIG/CXCL9 (*A* and *C*), and with SufA-degraded MIG/CXCL9 (*B* and *D*) at a concentration of 0.36 μM for 1 h at 37 °C. Following incubation, the bacteria were prepared for ultrathin sectioning/immunoelectron microscopy. Sections were incubated with polyclonal rabbit anti-human MIG/CXCL9 (1 μg/ml), followed by goat anti-rabbit IgG (1 μg/ml) labeled with colloidal gold (10 nm). The *bar* represents 100 nm.

Characterization of MIG/CXCL9 Fragments Generated by SufA—To identify the cleavage site(s) in MIG/CXCL9, recombinant chemokine was subjected to proteolysis by SufA. Following incubation for 3 h, cleavage products were separated on SDS-PAGE showing that multiple fragments of MIG/CXCL9 had been generated (Fig. 3*A*). Cleavage was a fast process and already after 5 min of incubation, fragments were generated (data not shown). Recombinant MIG/CXCL9 also appeared in a dimeric form, which is commonly observed even in the presence of strong reducing agents (Fig. 3*A*). Such dimers were not observed in Western blot (Fig. 2), which could be explained by hidden epitopes in the dimer or the lower concentration of the chemokine used in this experiment. The protein bands corresponding to the SufA-generated MIG/CXCL9 fragments were excised and subjected to MS and MS/MS analysis (Fig. 3*A*). The obtained peptide sequences demonstrated that SufA cleaves at sites in the COOH-terminal region

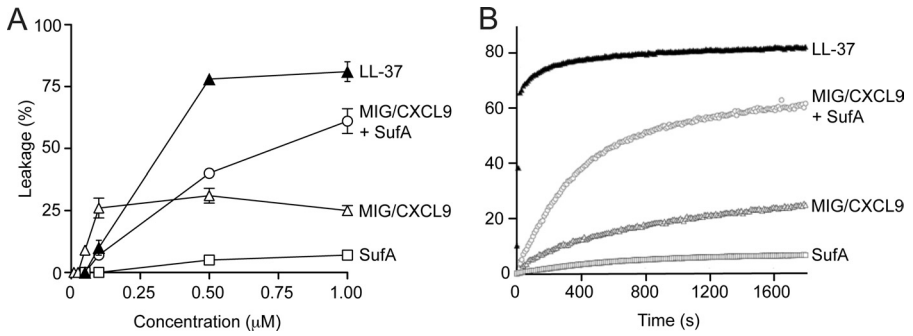

FIGURE 6. **MIG/CXCL9 causes liposome leakage.** Membrane-disruptive effects of intact MIG/CXCL9, SufA-degraded MIG/CXCL9, SufA alone, and LL-37 were analyzed by measuring the release of CF from liposomes. *A*, leakage induced by various peptide concentrations in 10 mM Tris-HCl buffer, pH 7.4, containing 5 mM glucose. *B*, kinetics of peptide induced liposome leakage. At time $t = 0$ s, 1 μM peptide was added.

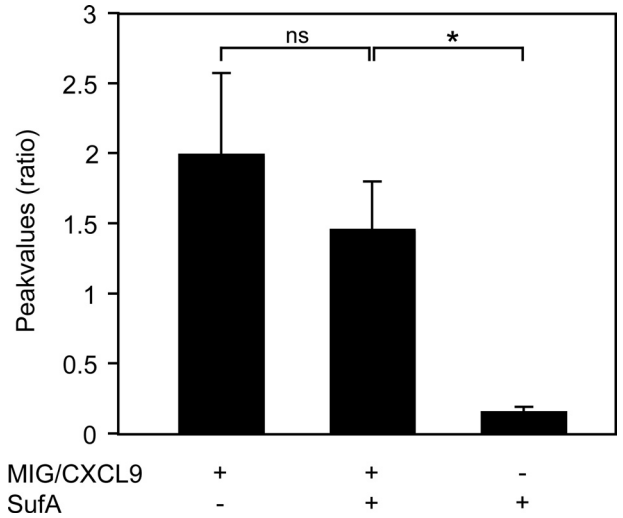

FIGURE 7. **SufA-degraded MIG/CXCL9 activates CXCR3.** The murine pre-B cell line L1.2, stably expressing the human MIG/CXCL9 receptor CXCR3, was loaded with a calcium-sensitive fluorophore. The rise in intracellular [Ca^{2+}] was analyzed after application of the peptide. *Lane 1*, MIG/CXCL9 (100 nM); *lane 2*, SufA-degraded MIG/CXCL9 (MIG/CXCL9 100 nM; SufA 1.5 nM); *lane 3*, SufA (1.5 nM). Data are represented as mean peak values ± S.D. values from three separate experiments.

of the MIG/CXCL9 peptide (Fig. 3*C*). The results also indicate that cleavage occurs in the NH_2-terminal part. Although of various lengths, all fragments contained the previously identified bactericidal region of MIG/CXCL9, located in the proximal part of the putative amphiphatic α-helix of the COOH terminus (10). A predictive structure of MIG/CXCL9 with the sites prone to SufA cleavage is shown in Fig. 3*B*.

SufA Generated MIG/CXCL9 Fragments Show Low Antibacterial Activity against F. magna but Retain Their Activity against S. pyogenes—It has been shown that SufA proteolysis of MIG/CXCL9 generates fragments that are inactive against *F. magna* (17). To test whether this is the case also for *S. pyogenes,* a bactericidal assay was performed. The *S. pyogenes* AP1 strain and the *F. magna* strain 505 were incubated with uncleaved and SufA-digested MIG/CXCL9, respectively. Strikingly, SufA-generated MIG/CXCL9 fragments efficiently killed AP1 bacteria, while 505 bacteria were unaffected at equimolar concentrations as judged by the viable counts assay (Fig. 4). Because of interfering activity of the medium used for cultivation of the HaCaT cells the bactericidal activity of MIG/CXCL9 produced by the keratinocytes could not be tested.

Bacteria from the two strains, incubated with MIG/CXCL9 or SufA-degraded MIG/CXCL9 respectively, were also analyzed by immunoelectron microscopy. Immunogold labeling of bacteria exposed to intact MIG/CXCL9, revealed presence of the chemokine both on the membrane and in the cytoplasm of 505 and AP1 bacteria. Furthermore, the bacterial morphology was affected by the chemokine as visualized by an irregular and less electron dense cytoplasmatic appearance (Fig. 5, *A* and *C*). In contrast, SufA-processed MIG/CXCL9 was detected only in the cytoplasm of AP1 bacteria but not in the 505 strain (Fig. 5*D*). In the case of the 505 strain, the processed chemokine was identified solely at the bacterial surface and the bacteria appeared unaffected by the MIG/CXCL9 fragments (Fig. 5*B*). These data support the results of the bactericidal assay in that they demonstrate that cleavage of MIG/CXCL9 by SufA provides a selective advantage for *F. magna* compared with *S. pyogenes*.

To further investigate the effect of MIG/CXCL9 on membranes, the holopeptide and SufA-degraded MIG/CXCL9 respectively, were tested for induction of liposome leakage. SufA alone did not cause any appreciable leakage, which is not unexpected, given the low concentration of the enzyme (<0.35 ng/ml in the cuvette) (Fig. 6, *A* and *B*). Surprisingly, SufA-digested MIG/CXCL9 displayed higher capacity to induce leakage than intact MIG/CXCL9, which had a quite low membrane-disruptive effect also at high concentrations (Fig. 6, *A* and *B*). However, intact MIG/CXCL9 induced somewhat higher leakage in liposomes at low concentrations. These unexpected results might be explained by dimerization and oligomerization of intact MIG/CXCL9 at higher concentrations (see Fig. 3*A*), resulting in different membrane-disruptive effect on bacteria and liposomes, possibly due to roles played by non-lipid components in bacterial walls, such as peptidoglycan and lipoteichoic acid. For all three samples, liposome leakage was significantly lower than that of the classical and important human antibacterial peptide LL-37. As judged from circular dichroism, MIG/CXCL9 contains α-helical motif(s), although no quantification of the helix content was made. As compared with the holoprotein there was no significant structural change in SufA-degraded MIG/CXCL9. In addition, no helix induction or any other secondary structural change of intact or SufA-degraded MIG/CXCL9 could be detected in the presence of liposomes (data not shown).

MIG/CXCL9 Fragments Activate the MIG/CXCL9 Receptor CXCR3—Upon binding MIG/CXCL9 activates the G-protein-coupled receptor CXCR3 that is expressed on eosinophils, NK cells, activated T cells, and endothelial cells. Binding to the receptor causes G-protein-dependent activation of calcium channels, resulting in influx of extracellular calcium (8). To investigate if MIG/CXCL9 processed by SufA retains its

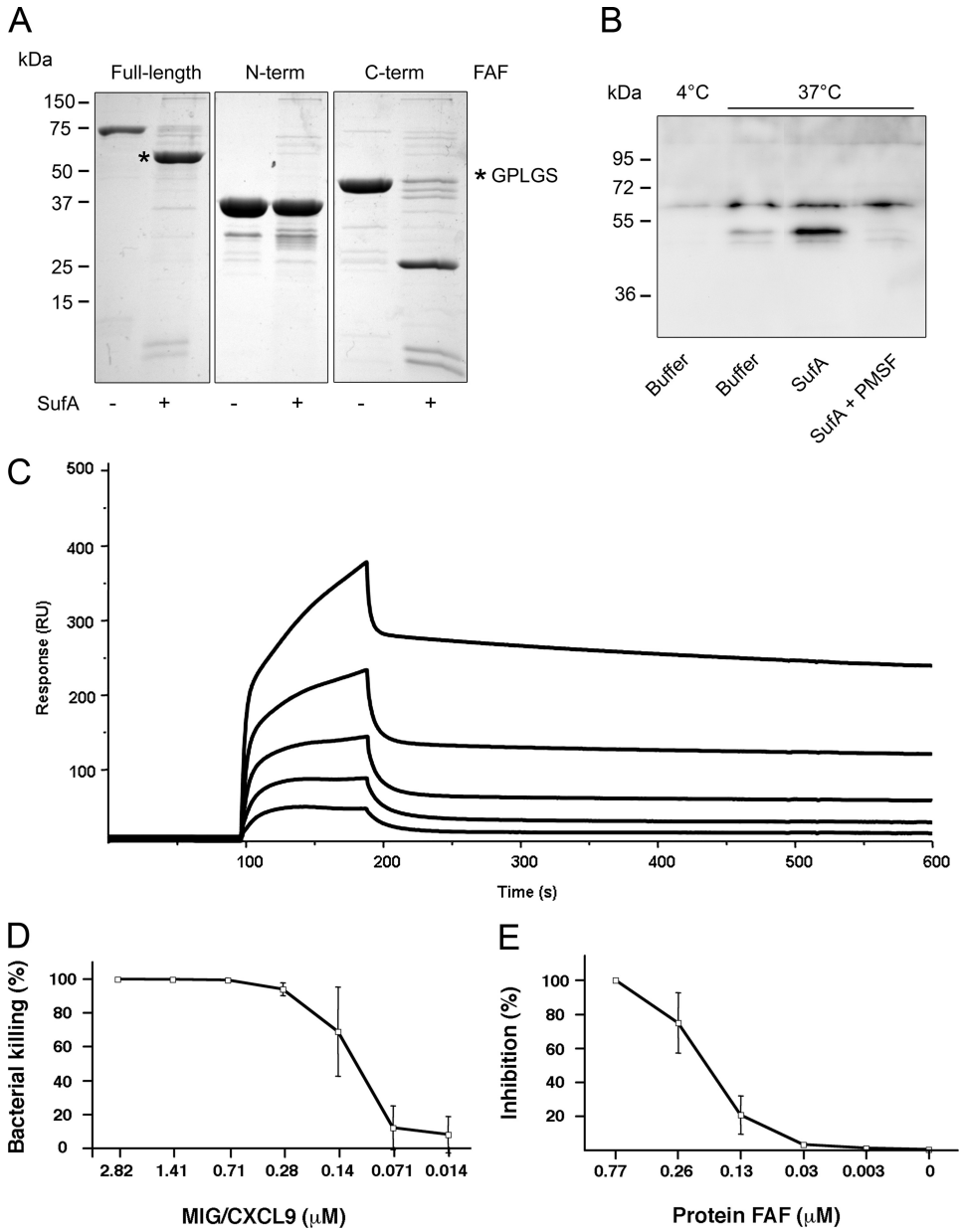

FIGURE 8. **SufA releases an NH_2-terminal fragment of FAF from the ALB8 surface.** *A*, 10 μg of recombinant full-length FAF, and the NH_2-terminal and COOH-terminal FAF fragments, respectively, were incubated with SufA (100 ng) or buffer for 18 h at 37 °C and then separated by SDS-PAGE. The band indicated with a *star* was excised and subjected to NH_2-terminal amino acid sequencing. The sequence obtained (GPLSG) corresponds to the residual amino acids of GST, in fusion with the NH_2 terminus of FAF, following Prescission proteinase removal of the GST tag. *B*, ALB8 bacteria were washed in 20 mM Tris-HCl, pH 7.5, and adjusted to 2×10^9 cfu/ml. Bacteria were incubated at 4 °C with buffer or at 37 °C with buffer, 0.5 μg SufA, or SufA+PMSF (5 mM) for 3 h, and then vortexed and centrifuged. The resulting supernatants were separated by SDS-PAGE and blotted to an Immobilon-P membrane. FAF was detected with polyclonal rabbit anti-FAF antiserum (1:1000). *C*, investigation of the affinity between MIG/CXCL9 and protein FAF utilizing surface plasmon resonance. Protein FAF was immobilized and MIG/CXCL9 at concentrations ranging from 30–500 nM was injected over the surface of the chip. The affinity was determined to 4.9 nM. *D*, bactericidal effect of MIG/CXCL9 at various concentrations was tested against *F. magna* 505 (2×10^6 cfu/ml). Following incubation for 1 h at 37 °C, cfus were determined. Data are represented as mean ± S.D. values from three separate experiments. *E*, bactericidal effect of MIG/CXCL9 at a concentration of 0.28 μM was inhibited with various concentrations of protein FAF. Data are represented as mean ± S.D. values from three separate experiments.

CXCR3-activating properties, murine pre-B cells transfected with CXCR3 were used. The cells were loaded with a calcium-sensitive fluorophore (FURA-2) followed by exposure to intact and SufA-processed MIG/CXCL9, respectively. In both cases, an influx of calcium was seen, reflecting activation of the receptor (Fig. 7). As a control, MIG/CXCL9 did not induce calcium influx in non-transfected cells (data not shown).

Protein FAF Released by SufA Binds to and Inactivates MIG/CXCL9—The surface protein FAF mediates adhesion of *F. magna* through an interaction with BM-40, a protein present in basement membranes and in the epidermis (15). In addition to being surface-associated, a fragment of FAF is also released in substantial quantities into the growth medium of *F. magna*. Moreover, FAF blocks the activity of the antibacterial peptide LL-37 (15). To determine if SufA can cleave FAF, recombinant preparations of full-length FAF, an NH_2-terminal and a COOH-terminal fragment of FAF were incubated with SufA for 18 h at 37 °C. Analysis by SDS-PAGE showed that cleavage occurs in the COOH-terminal part of FAF (Fig. 8*A*), suggesting that the enzyme can release the protein from the bacterial surface. Similar results were obtained with an incubation time of 1 h (results not shown). Next, we investigated whether SufA releases FAF from the bacterial surface. ALB8 bacteria incubated at 37 °C spontaneously released fragments interacting with antibodies against FAF as detected by Western blot. Exogenously added SufA resulted in an increased FAF release that was blocked by the serine proteinase inhibitor PMSF (Fig. 8*B*). The results demonstrate that SufA can release FAF from the surface of the bacteria. However, additional proteolytic activity is likely to be involved, since shedding resulting in similar FAF fragments was observed in growth medium from the CK05 strain, lacking active SufA (data not shown).

To analyze a possible interaction between FAF and MIG/CXCL9, surface plasmon resonance spectrometry was utilized. MIG/CXCL9 was immobilized on a sensor chip and protein FAF bound MIG/CXCL9 with high affinity (Fig. 8*C*). We then investigated the inhibitory effect of FAF on MIG/CXCL9 killing of *F. magna*. In this assay, strain 505, which does not carry the *faf*-gene, was used. At a bactericidal concentration of MIG/CXCL9 (0.28 μM,

Fig. 8*D*) FAF was found to dose-dependently block the antibacterial activity of the chemokine (Fig. 8*E*).

DISCUSSION

This study shows that SufA, released by *F. magna*, can cleave the antibacterial chemokine MIG/CXCL9, rendering the molecule less active as an antibacterial agent but retaining its receptor-activating activity against the CXCR3 receptor that is involved in suppression of angiogenesis.

F. magna colonizes the human oro-pharynx and skin, habitats where the virulent human pathogen *S. pyogenes* has a preference for causing infections, such as tonsillitis and erysipelas respectively (30). High expression of MIG/CXCL9 is seen both in skin and in the oro-pharynx during inflammation and, as a consequence, *F. magna* and *S. pyogenes* are likely to encounter this antibacterial chemokine concurrently during infection *in vivo* (10, 31). In contrast to the virulent pathogen *S. pyogenes*, *F. magna* did not increase the production of MIG/CXCL9 in IFN-γ stimulated keratinocytes. The reason for this may be that pathogen-associated molecular patterns (PAMPs; *e.g.* peptidoglycan and lipoteichoic acid) are less exposed on the surface of *F. magna*. PAMPs are recognized by receptors of the innate immune system, not least the TLRs. TLRs activate the proinflammatory transcription factor NF-κB, resulting in increased expression of MIG/CXCL9 (29). Thus, *F. magna* seem less prone to evoke an inflammatory response, thereby promoting its survival as a commensal during non-inflammatory conditions.

In a previous study, the antibacterial activity of MIG/CXCL9 was mapped to the prominent COOH-terminal α-helix of the molecule (10). Interestingly, the antibacterial function of SufA-cleaved MIG/CXCL9 is affected although a large portion of this antibacterial motif is preserved. The exact mechanism by which MIG/CXCL9 executes bacterial killing is not known. In this study, electron microscopy revealed that MIG/CXCL9, in addition to its membrane-perturbation properties, is translocated over the bacterial membrane entering the cytoplasm (see Fig. 5), possibly inhibiting enzymatic activities including metabolism. This notion is also supported by the seemingly contradictory effects from SufA cleavage of MIG/CXCL9, observed on bacteria and model liposomes, suggesting more complex mechanisms than lipid membrane disintegration. Such mechanisms have been described for other antimicrobial peptides (32). Interestingly, SufA-cleaved MIG/CXCL9 only entered the cytoplasm of *S. pyogenes* but not that of *F. magna*. It has been demonstrated that the ability to form oligomers is essential for the activity of many chemokines (33, 34). Under denaturing conditions, MIG/CXCL9 still forms dimers, but this was not observed with the SufA-processed chemokine (see Fig. 3*A*). Thus, the shortening of the NH_2 and COOH terminus in SufA-cleaved MIG/CXCL9 can result in a decreased tendency to oligomerize which may in part explain its reduced antibacterial potency against *F. magna*. In contrast, SufA-cleaved MIG/CXCL9 was still active against *S. pyogenes*, suggesting that differences in cell wall architecture between these bacterial species also could play a role in the different sensitivity toward the processed chemokine. Finally, differences in membrane composition could contribute to the observed chemokine effects on *F. magna* and *S. pyogenes*.

The NH_2 terminus of chemokines contains disulfide bonds that stabilize the three anti-parallel β-sheets. These are considered important for receptor-activation (6). However, studies on the interaction of MIG/CXCL9 with the CXCR3 receptor showed that neither the first 73 amino acids, nor amino acids 74–103 of MIG/CXCL9 could alone activate the receptor, but that the holopeptide including the COOH terminus was necessary (35). The findings of the present study on the other hand, indicates that neither the full COOH terminus, nor the full NH_2 terminus, is critical for receptor activation. It may seem paradoxical that the receptor-activating activity of MIG/CXCL9 is left unaffected by SufA proteolysis, thus possibly counteracting the survival of the bacterium. However, MIG/CXCL9 is a potent inhibitor of angiogenesis, an effect mediated by CXCR3 expressed on the endothelium (8, 36). Since *F. magna* is an anaerobic bacterium, lowering the oxygen saturation of surrounding tissues by suppression of angiogenesis, may further promote its survival as compared with aerobic bacteria.

The majority of *F. magna* isolates express the surface protein FAF, that mediates bacterial adhesion to epidermis and basement membranes (15). SufA promotes release of FAF from the bacterial surface, resulting in binding to and neutralization of the antibacterial activity of MIG/CXCL9 "on a distance." In addition, it has also been demonstrated that FAF interferes with the activity of the antibacterial peptide LL-37 (15). Thus, FAF, released by SufA, could protect *F. magna* from the effects of both MIG/CXCL9 and LL-37 present in the environment.

Taken together, SufA-mediated modulation of inflammatory effector molecules, in particular MIG/CXCL9, provides means by which *F. magna* can decrease antibacterial activity and suppress angiogenesis, during inflammation. This can create an ecologic niche for *F. magna* and enhance bacterial survival during infections caused by virulent pathogens such a *S. pyogenes*.

Acknowledgments—We thank Pia Andersson, Maria Baumgarten, and Lise-Britt Wahlberg for excellent technical assistance. Dr. Mattias Collin is acknowledged for providing the homology model of MIG/CXCL9.

REFERENCES

1. Tlaskalová-Hogenová, H., Stepánková, R., Hudcovic, T., Tucková, L., Cukrowska, B., Lodinová-Zádníková, R., Kozáková, H., Rossmann, P., Bártová, J., Sokol, D., Funda, D. P., Borovská, D., Reháková, Z., Sinkora, J., Hofman, J., Drastich, P., and Kokesová, A. (2004) *Immunol. Lett.* **93,** 97–108
2. Higaki, S., and Morohashi, M. (2003) *Drugs Exp. Clin. Res.* **29,** 153–155
3. Murdoch, D. A. (1998) *Clin. Microbiol. Rev.* **11,** 81–120
4. Bowler, P. G., Duerden, B. I., and Armstrong, D. G. (2001) *Clin. Microbiol. Rev.* **14,** 244–269
5. Stephens, P., Wall, I. B., Wilson, M. J., Hill, K. E., Davies, C. E., Hill, C. M., Harding, K. G., and Thomas, D. W. (2003) *Br. J. Dermatol.* **148,** 456–466
6. Baggiolini, M. (2001) *J. Intern. Med.* **250,** 91–104
7. Liao, F., Rabin, R. L., Yannelli, J. R., Koniaris, L. G., Vanguri, P., and Farber, J. M. (1995) *J. Exp. Med.* **182,** 1301–1314
8. Loetscher, M., Gerber, B., Loetscher, P., Jones, S. A., Piali, L., Clark-Lewis, I., Baggiolini, M., and Moser, B. (1996) *J. Exp. Med.* **184,** 963–969
9. Cole, A. M., Ganz, T., Liese, A. M., Burdick, M. D., Liu, L., and Strieter, R. M. (2001) *J. Immunol.* **167,** 623–627
10. Egesten, A., Eliasson, M., Johansson, H. M., Olin, A., Mörgelin, M., Muel-

ler, A., Pease, J. E., Frick, I. M., and Björck, L. (2007) *J. Infect. Dis.* **195,** 684–693
11. Romagnani, P., Annunziato, F., Lasagni, L., Lazzeri, E., Beltrame, C., Francalanci, M., Uguccioni, M., Galli, G., Cosmi, L., Maurenzig, L., Baggiolini, M., Maggi, E., Romagnani, S., and Serio, M. (2001) *J. Clin. Invest.* **107,** 53–63
12. Eliasson, M., Frick, I. M., Collin, M., Sørensen, O. E., Björck, L., and Egesten, A. (2007) *Microb. Pathog.* **43,** 224–233
13. Engelhardt, E., Toksoy, A., Goebeler, M., Debus, S., Bröcker, E. B., and Gillitzer, R. (1998) *Am. J. Pathol.* **153,** 1849–1860
14. Sauty, A., Dziejman, M., Taha, R. A., Iarossi, A. S., Neote, K., Garcia-Zepeda, E. A., Hamid, Q., and Luster, A. D. (1999) *J. Immunol.* **162,** 3549–3558
15. Frick, I. M., Karlsson, C., Mörgelin, M., Olin, A. I., Janjusevic, R., Hammarström, C., Holst, E., de Château, M., and Björck, L. (2008) *Mol. Microbiol.* **70,** 695–708
16. Potempa, J., and Pike, R. N. (2009) *J. Innate Immun.* **1,** 70–87
17. Karlsson, C., Andersson, M.-L., Collin, M., Schmidtchen, A., Björck, L., and Frick, I.-M. (2007) *Microbiology* **153,** 4208–4218
18. Karlsson, C., Mörgelin, M., Collin, M., Lood, R., Andersson, M.-L., Schmidtchen, A., Björck, L., and Frick, I.-M. (2009) *Microbiology* **155,** 238–248
19. Boukamp, P., Petrussevska, R. T., Breitkreutz, D., Hornung, J., Markham, A., and Fusenig, N. E. (1988) *J. Cell Biol.* **106,** 761–771
20. Dahlgren, C., Christophe, T., Boulay, F., Madianos, P. N., Rabiet, M. J., and Karlsson, A. (2000) *Blood* **95,** 1810–1818
21. Laemmli, U. K. (1970) *Nature* **227,** 680–685
22. Schägger, H., and von Jagow, G. (1987) *Anal. Biochem.* **166,** 368–379
23. Påhlman, L. I., Olin, A. I., Darenberg, J., Mörgelin, M., Kotb, M., Herwald, H., and Norrby-Teglund, A. (2008) *Cell. Microbiol.* **10,** 404–414
24. Fernandez-Fuentes, N., Madrid-Aliste, C. J., Rai, B. K., Fajardo, J. E., and Fiser, A. (2007) *Nucleic Acids Res.* **35,** W363–368
25. Malkowski, M. G., Lazar, J. B., Johnson, P. H., and Edwards, B. F. (1997) *J. Mol. Biol.* **266,** 367–380
26. Humphrey, W., Dalke, A., and Schulten, K. (1996) *J. Mol. Graph.* **14,** 33–38, 27–28
27. Stone, J. (1998) *Masters Thesis*, Computer Science Department, University of Missouri-Rolla
28. Carlemalm, E., and Villiger, W. (1989) in *Techniques in Immunocytochemistry* (Bullbock, G. R., and Petrusz, P. eds), Academic Press, London
29. Ohmori, Y., Schreiber, R. D., and Hamilton, T. A. (1997) *J. Biol. Chem.* **272,** 14899–14907
30. Cunningham, M. W. (2000) *Clin. Microbiol. Rev.* **13,** 470–511
31. Goebeler, M., Toksoy, A., Spandau, U., Engelhardt, E., Bröcker, E. B., and Gillitzer, R. (1998) *J. Pathol.* **184,** 89–95
32. Brogden, K. A. (2005) *Nat. Rev. Microbiol.* **3,** 238–250
33. Campanella, G. S., Grimm, J., Manice, L. A., Colvin, R. A., Medoff, B. D., Wojtkiewicz, G. R., Weissleder, R., and Luster, A. D. (2006) *J. Immunol.* **177,** 6991–6998
34. Proudfoot, A. E., Handel, T. M., Johnson, Z., Lau, E. K., LiWang, P., Clark-Lewis, I., Borlat, F., Wells, T. N., and Kosco-Vilbois, M. H. (2003) *Proc. Natl. Acad. Sci. U.S.A.* **100,** 1885–1890
35. Clark-Lewis, I., Mattioli, I., Gong, J. H., and Loetscher, P. (2003) *J. Biol. Chem.* **278,** 289–295
36. Strieter, R. M., Polverini, P. J., Kunkel, S. L., Arenberg, D. A., Burdick, M. D., Kasper, J., Dzuiba, J., Van Damme, J., Walz, A., Marriott, D., Chan, S.-Y., Roczniak, S., and Shanafelt, A. B. (1995) *J. Biol. Chem.* **270,** 27348–27357